

A simple schematic model for a cross section deficit in $^{12}\text{C}+^{12}\text{C}$ fusion reactions

K. Hagino

Department of Physics, Kyoto University, Kyoto 606-8502, Japan

A cross section deficit phenomenon has been observed in $^{12}\text{C}+^{12}\text{C}$ fusion reactions at astrophysical energies, at which fusion cross sections are suppressed in the off-resonance regions as compared to fusion cross sections for the $^{12}\text{C}+^{13}\text{C}$ system. I here construct a simple schematic model which simulates this phenomenon. The model consists of a random matrix Hamiltonian based on the Gaussian Orthogonal Ensemble (GOE), which is coupled to an entrance channel Hamiltonian in the discrete basis representation. I show that the transmission coefficients are almost unity when both the level density and the decay widths of the GOE configurations are large, realizing the strong absorption regime. On the other hand, when these parameters are small, the transmission coefficients are significantly structured as a function of energy. In that situation, the transmission coefficients at resonance energies reach unity in this model, that is consistent with the experimental finding of the cross section deficit.

I. INTRODUCTION

The $^{12}\text{C}+^{12}\text{C}$ fusion reaction at extremely low energies has attracted lots of attention both experimentally and theoretically [1–21], largely because this is one of the key reactions in nuclear astrophysics. This reaction is important e.g., in carbon burning in massive stars, type Ia supernovae, and X-ray superburst. A characteristic feature of the fusion cross sections of this system is that there are many prominent resonance peaks. This is in contrast to fusion cross sections of a similar system, the $^{12}\text{C}+^{13}\text{C}$ fusion reaction, which show a much smoother energy dependence of cross sections. Another interesting observation is that the fusion cross sections of the $^{12}\text{C}+^{12}\text{C}$ reaction at resonance energies appear to coincide with the cross sections of the $^{12}\text{C}+^{13}\text{C}$ reaction, while those at off-resonance energies are relatively suppressed [5, 6]. That is, the fusion cross sections of the $^{12}\text{C}+^{13}\text{C}$ reaction seem to provide the upper limit of the fusion cross sections of the $^{12}\text{C}+^{12}\text{C}$ system. This was referred to as a cross section deficit in Ref. [10]. Its mechanism has not yet been completely clarified.

It was argued in Ref. [10] that the different behaviors of fusion cross sections in these systems are caused by i) a lower Q -value of the $^{12}\text{C}+^{12}\text{C}$ fusion reaction as compared to the Q value of the $^{12}\text{C}+^{13}\text{C}$ fusion reaction, ii) the compound nucleus formed in the $^{12}\text{C}+^{12}\text{C}$ fusion reaction is ^{24}Mg , that is an even-even nucleus and thus the level density is lower than that of ^{25}Mg formed in the $^{12}\text{C}+^{13}\text{C}$ reaction, and iii) $^{12}\text{C}+^{12}\text{C}$ is a reaction of identical bosons so that only states with positive parity and even spin in ^{24}Mg can be populated. All of these lead to the fact that resonances are isolated in the $^{12}\text{C}+^{12}\text{C}$ fusion reaction at low energies, while the $^{12}\text{C}+^{13}\text{C}$ fusion reaction is in the overlapping resonance regime even at low energies. In the former case, it is known that average transmission coefficients are suppressed by the Moldauer factor, $P_J = 1 - e^{-2\pi\Gamma_J/D_J}$, where J is the spin of the compound nucleus, Γ_J is the average decay width, and D_J is the average level spacing [10, 22–24]. See also Refs. [25, 26] for the derivation of the Moldauer factor. Notice

that the low Q -value of the the $^{12}\text{C}+^{12}\text{C}$ fusion reaction also leads to the fact that the neutron emission channel from the compound nucleus is closed in the $^{12}\text{C}+^{12}\text{C}$ fusion reaction, while such channel is open in the $^{12}\text{C}+^{13}\text{C}$ fusion reaction.

The Moldauer factor explains why the fusion cross sections of the $^{12}\text{C}+^{12}\text{C}$ system are suppressed on average as compared to the cross sections of the $^{12}\text{C}+^{13}\text{C}$ system. However, it does not provide a reasoning why the fusion cross sections of the $^{12}\text{C}+^{12}\text{C}$ system at the resonance energies coincide with the cross sections of the $^{12}\text{C}+^{13}\text{C}$ system. To address this question, in this paper I consider a simple schematic model which was used in Appendix B of Ref. [27]. The model consists of a random matrix Hamiltonian based on the Gaussian Orthogonal Ensemble (GOE) which is coupled to scattering states in the entrance channel. Each of the GOE configurations possess a decay width γ so that a part of the incident flux is absorbed by the GOE configurations. By changing the parameters in the GOE Hamiltonian and the decay width γ , one can simulate both the isolated resonance regime and the overlapping resonance regime, and thus the model provides a convenient tool to qualitatively understand the difference in the fusion cross sections of the two C+C systems.

The paper is organized as follows. In Sec. II, I detail the simple schematic model which is employed in this paper. In particular, I explain in detail how one can compute the transmission coefficients, or the absorption probabilities, based on the discrete basis formalism. In Sec. III, I compare the isolated resonance regime and the overlapping resonance regime with this model and show that the model can qualitatively reproduce the experimental findings in the C+C fusion reactions. I then summarize the paper in Sec. IV. In the Appendix, I detail a numerical method to compute poles of the S -matrix in the complex energy plane.

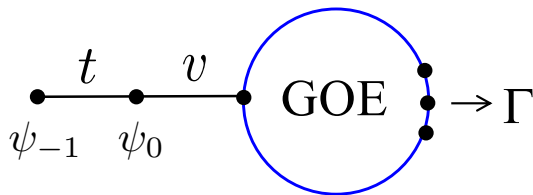


FIG. 1: A schematic illustration of the model Hamiltonian employed in this paper. It consists of a random matrix based on the Gaussian Orthogonal Ensemble (GOE), which is coupled to the free scattering states ψ_i with the strength v . Γ is the decay width of the GOE configurations, while t denotes the off-diagonal component of the kinetic energy operator, which connects neighboring scattering states in the discrete basis representation.

II. MODEL

The model employed in this paper is schematically illustrated in Fig. 1. This is the same model as that in Appendix B in Ref. [27], and consists of a GOE Hamiltonian H_{GOE} with the dimension of N_{GOE} . The matrix elements of the GOE Hamiltonian read,

$$(H_{\text{GOE}})_{ij} = v_g r_{ij} \sqrt{1 + \delta_{i,j}}, \quad (1)$$

where v_g is the average strength of the interaction and r_{ij} is a random number from a Gaussian distribution of unit dispersion, $\langle r_{ij}^2 \rangle = 1$. I assume that the first N_{decay} basis states have a decay width of γ . Thus the total GOE Hamiltonian is given by

$$H'_{\text{GOE}} = H_{\text{GOE}} - \frac{i}{2}\Gamma, \quad (2)$$

where Γ is a diagonal matrix in which the first N_{decay} components are γ and the rest is zero.

In Fig. 1, ψ_0 and ψ_{-1} represent free scattering wave functions at x_0 and x_{-1} ($= x_0 - \Delta x$), respectively, Δx being the mesh spacing. The free scattering wave functions satisfy the equation

$$t\psi_{i-1} + t\psi_{i+1} = (E' + 2t)\psi_i \equiv E\psi_i, \quad (3)$$

where ψ_i is the wave function at x_i . Here the scattering energy E' is shifted as $E = E' + 2t$ so that the diagonal component of the kinetic energy operator, $-2t$, does not appear in the equation. Assuming the plane wave solution, $\psi_i \propto e^{\pm ikx_i}$, one finds that the relation between E and k is given by

$$E = 2t \cos(k\Delta x). \quad (4)$$

I assume that the free wave function ψ_0 couples to the first basis state of the GOE Hamiltonian with the strength v . Thus, the wave functions ψ_0 and ψ_{-1} , as well

as the amplitudes $\{f_i\}$ for the GOE basis states satisfy the equation

$$\begin{pmatrix} 0 & \vec{v}^T \\ \vec{v} & H'_{\text{GOE}} \end{pmatrix} \begin{pmatrix} \psi_0 \\ \vec{f} \end{pmatrix} = E \begin{pmatrix} \psi_0 \\ \vec{f} \end{pmatrix} + \begin{pmatrix} -t\psi_{-1} \\ \vec{0} \end{pmatrix}, \quad (5)$$

where the N_{GOE} -component vectors $\vec{0}$ and \vec{v} are defined as $\vec{0} = (0, 0, \dots, 0)^T$ and $\vec{v} = (v, 0, \dots, 0)^T$, respectively. Here, T denotes the transpose. By taking the last N_{GOE} rows in Eq. (5),

$$(H'_{\text{GOE}} - E)\vec{f} = \begin{pmatrix} -v\psi_0 \\ 0 \\ \vdots \\ 0 \end{pmatrix}, \quad (6)$$

the amplitudes \vec{f} can be obtained as a ratio to ψ_0 as [28, 32]

$$f_i = -(H'_{\text{GOE}} - E)^{-1}_{i1} v\psi_0 \equiv -G_{i1} v\psi_0, \quad (7)$$

where $G \equiv (H'_{\text{GOE}} - E)^{-1}$ is the Green function. After the amplitudes \vec{f} are so obtained, the wave function ψ_{-1} is obtained as

$$\psi_{-1} = -\frac{1}{t}(-E\psi_0 + v f_1) = -\frac{\psi_0}{t}(-E - G_{11}v^2). \quad (8)$$

Since ψ_0 and ψ_{-1} represent the free scattering wave functions, they should satisfy the relation

$$\psi_{-1} = A(e^{-ik\Delta x} - S e^{ik\Delta x}), \quad (9)$$

$$\psi_0 = A(1 - S), \quad (10)$$

where S is the S -matrix. From these equations, the S -matrix reads,

$$S = \frac{\psi_{-1} - e^{-ik\Delta x}\psi_0}{\psi_{-1} - e^{ik\Delta x}\psi_0} = \frac{E + G_{11}v^2 - te^{-ik\Delta x}}{E + G_{11}v^2 - te^{ik\Delta x}}. \quad (11)$$

From the S -matrix, the absorption probability, or the transmission coefficient, is obtained as

$$T = 1 - |S|^2. \quad (12)$$

III. ROLE OF GOE PROPERTIES IN TRANSMISSION COEFFICIENTS

Let us now numerically evaluate the transmission coefficients and discuss the role played by the parameters in the GOE Hamiltonian. The red solid and the blue dashed lines in Fig. 2 show the transmission coefficients obtained with a single random seed for the parameters $(N_{\text{GOE}}, \gamma) = (100, 0.6)$ and $(N_{\text{GOE}}, \gamma) = (40, 0.05)$, respectively. To this end, I set $N_{\text{decay}} = N_{\text{GOE}}$ and take $v_g = 0.1$, $t = -1$, and $v = 1$. Notice that the transmission coefficients drop to zero at $E = \pm 2$, because the absolute value of energy E cannot be larger than $2t$ due

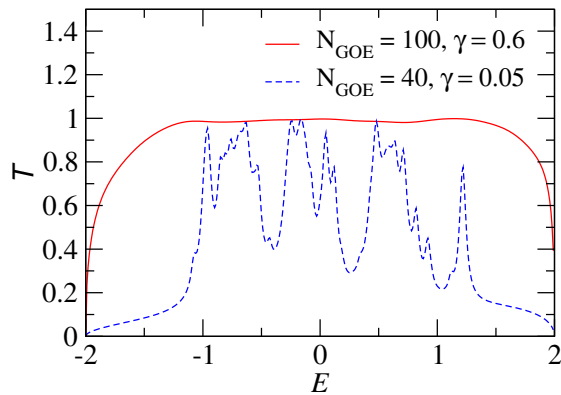


FIG. 2: Transmission coefficients obtained with a single random seed. The red solid and the blue dashed lines are obtained with $(N_{\text{GOE}}, \gamma) = (100, 0.6)$ and $(N_{\text{GOE}}, \gamma) = (40, 0.05)$, respectively. The number of decay channel, N_{decay} , is set to be $N_{\text{decay}} = N_{\text{GOE}}$ for each case. The other parameters are $v_g = 0.1$, $t = -1$, and $v = 1$.

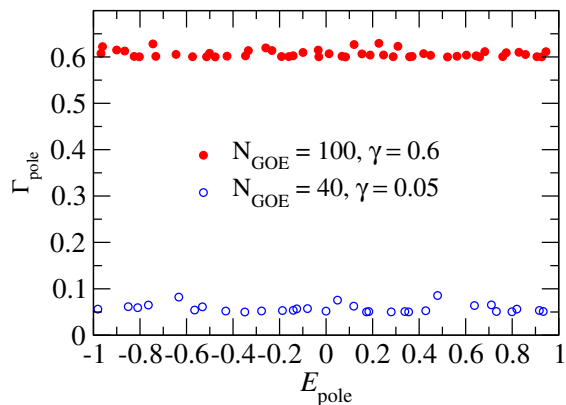


FIG. 3: The energies of the resonance poles, $E_{\text{pole}} - i\Gamma_{\text{pole}}/2$, corresponding to the two curves in Fig. 2.

to the dispersion relation, Eq. (4). Nevertheless, one can still discuss the behavior of the transmission coefficients around the central energy, $E \sim 0$. In the case of $(N_{\text{GOE}}, \gamma) = (100, 0.6)$, the transmission coefficients are close to unity. This is consistent with the strong absorption limit, which is often assumed in heavy-ion reactions [33, 34]. On the other hand, in the case of $(N_{\text{GOE}}, \gamma) = (40, 0.05)$, the transmission coefficients are much more structured as a function of E with several prominent resonance peaks. It is interesting to observe that the transmission coefficients are close to unity at a few resonance energies. This is similar to the cross section deficit observed in the $^{12}\text{C}+^{12}\text{C}$ reaction. The present simple model thus captures an essential feature of the C+C fusion reactions.

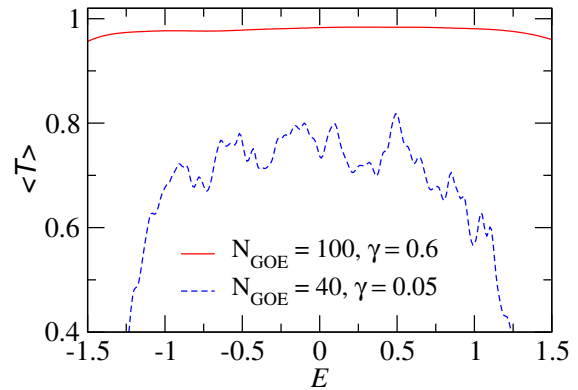


FIG. 4: An ensemble average of the transmission coefficients, $\langle T(E) \rangle = 1 - \langle |S(E)|^2 \rangle$, obtained with 20 ensembles. The parameters of the Hamiltonian are the same as those in Fig. 2.

The complex energies, $E_{\text{pole}} - i\Gamma_{\text{pole}}/2$, for the corresponding S -matrix poles are shown in Fig. 3. See Appendix for the numerical method to evaluate the resonance poles. The widths Γ_{pole} fluctuate around the unperturbed width, γ . The average level spacing is also close to the inverse of the level density of the GOE Hamiltonian, $\rho_{\text{GOE}} = \sqrt{N_{\text{GOE}}}/\pi v_g$. For $v_g = 0.1$, this is $1/\rho_{\text{GOE}} = 0.03$ and 0.05 for $N_{\text{GOE}} = 100$ and 40 , respectively. The value of γ is much larger than $1/\rho_{\text{GOE}}$ in the case of $(N_{\text{GOE}}, \gamma) = (100, 0.6)$, and the resonances are largely overlapping. As a consequence, the transmission coefficients show a smooth energy dependence as shown in Fig. 2. On the other hand, in the case of $(N_{\text{GOE}}, \gamma) = (40, 0.05)$, the value of γ is comparable to $1/\rho_{\text{GOE}}$, leading to the structured transmission coefficients.

An ensemble average of the transmission coefficients,

$$\langle T(E) \rangle = 1 - \langle |S(E)|^2 \rangle, \quad (13)$$

is shown in Fig. 4. To this end, I take an average of 20 ensembles. Because of the ensemble average, the structure of the blue dashed curve is significantly smeared as compared to that shown in Fig. 2 for a single random seed. Yet, one can still observe that the dashed line is much more structured than the solid line.

In the compound nucleus theory, the transmission coefficients obtained by an optical potential correspond to

$$\bar{T}(E) = 1 - |\langle S(E) \rangle|^2. \quad (14)$$

That is, the ensemble average is taken firstly for the S -matrix and then take the absolute value square to obtain the average transmission coefficients. If one decomposes the average transmission coefficients (13) as,

$$\langle T \rangle = 1 - |\langle S(E) \rangle|^2 - (\langle |S(E)|^2 \rangle - |\langle S(E) \rangle|^2), \quad (15)$$

$$= \bar{T} - (\langle |S(E)|^2 \rangle - |\langle S(E) \rangle|^2), \quad (16)$$

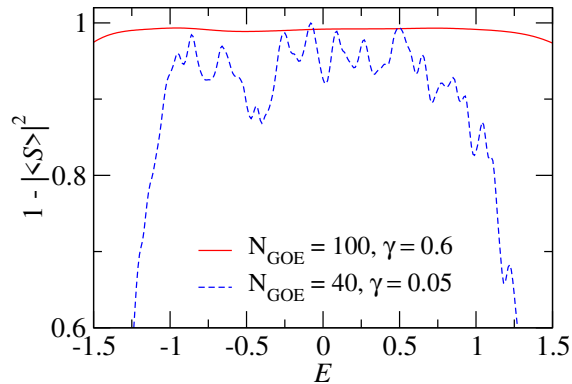


FIG. 5: The average transmission coefficients, $\bar{T}(E) = 1 - |\langle S(E) \rangle|^2$, obtained by firstly taking the ensemble average of the S -matrix.

\bar{T} corresponds to the probabilities of a compound nucleus formation, while the second term, $(\langle |S(E)|^2 \rangle - |\langle S(E) \rangle|^2)$, corresponds to the compound-elastic scattering [35]. The average transmission coefficients \bar{T} are plotted in Fig. 5. These transmission coefficients are qualitatively similar to the ensemble average of $T(E)$, even though the blue dashed line is somewhat increased. Interestingly, some of the resonance peaks are close to the solid line in the strong limit. Notice that the average transmission coefficients \bar{T} are the quantities which can be directly compared to the Moldauer factor, $1 - e^{-2\pi\Gamma\rho_{\text{GOE}}}$. If one uses $\Gamma = 0.05$ and $\rho_{\text{GOE}} = 1/0.05$ for $N_{\text{GOE}} = 40$, this factor is found to be 0.998. This deviates somewhat from the average transmission coefficients shown in Fig. 5, but this would be reasonable as the transmission coefficients would need to be small in order to validate the approximations used to derive the Moldauer factor [25, 26].

IV. SUMMARY

I have constructed a simple schematic model for a compound nucleus reaction and discussed the dependence of the transmission coefficients on the properties of the compound nucleus. The model consists of a random matrix based on the Gaussian Orthogonal Ensemble (GOE), which couples to a free scattering wave. By changing the dimension of the GOE Hamiltonian and the decay width of the compound nucleus states, the model can describe both the overlapping resonance regime and the isolated resonance regime. I have demonstrated that the transmission coefficients in the isolated resonance regime are suppressed at off-resonance energies as compared to the transmission coefficients in the overlapping resonance regime, which are close to unity. At on-resonance energies, the transmission coefficients in the isolated resonance regime are close to unity, exhibiting the deficit phenomenon at off-resonance energies. This is qualita-

tively the same as the experimental observations in the fusion cross sections of the $^{12}\text{C}+^{12}\text{C}$ and $^{12}\text{C}+^{13}\text{C}$ systems. Therefore, even though the present model is simple enough, it still captures an essential feature of the fusion reactions of two carbon nuclei.

The present model can be extended by replacing the GOE Hamiltonian by a more realistic many-body Hamiltonian, such as a shell model Hamiltonian. Such study will shed light on the dynamics of resonance reactions relevant to nuclear astrophysics, while keeping a quantitative description of the cross sections. I will report on this in a separate publication.

Acknowledgments

I thank G.F. Bertsch, X.D. Tang, A.B. Brown and K. Uzawa for useful discussions. This work was supported in part by JSPS KAKENHI Grant Number JP23K03414.

Appendix A: Poles of the S -matrix

To find the poles of the S -matrix, Eq. (11), in the complex plane, I closely follow the method in Supplemental Material of Ref. [28]. In this method, the outgoing boundary condition $\psi_0 = e^{-ik\Delta x}\psi_{-1}$ is imposed to the scattering wave functions, and an iterative procedure is introduced to find the poles. Substituting $\psi_{-1} = e^{ik\Delta x}\psi_0$ to Eq. (5), one finds

$$M(x)\vec{\psi} \equiv (H + te^{ik\Delta x}C - E)\vec{\psi} = 0, \quad (\text{A1})$$

where x is defined as $x \equiv k\Delta x$, and $\vec{\psi}$ and H are defined as $\vec{\psi} \equiv (\psi_0, \vec{f})^T$ and

$$H \equiv \begin{pmatrix} 0 & \vec{v}^T \\ \vec{v} & H'_{\text{GOE}} \end{pmatrix}, \quad (\text{A2})$$

respectively. C is a matrix with the elements of $C_{ij} = \delta_{i,j}\delta_{i,0}$.

If one takes an arbitrary number $x = x_g$, Eq. (A1) is not satisfied in general. However, one can improve x_g by assuming that it is close to x_r which satisfies Eq. (A1). From $M(x_r)\vec{\psi} = 0$ and $x_r = x_g + x_r - x_g$, one obtains

$$\left[M(x_g) + (x_r - x_g) \frac{dM}{dx} \Big|_{x_g} \right] \vec{\psi} = 0, \quad (\text{A3})$$

up to the first order of $x_r - x_g$. This equation is transformed to

$$(M'(x_g))^{-1}M(x_g)\vec{\psi} = (x_g - x_r)\vec{\psi}. \quad (\text{A4})$$

Since the right-hand side of this equation vanishes for resonance poles, one can take the lowest modulus eigenvalue $\bar{\lambda}$ of $(M'(x_g))^{-1}M(x_g)$ and update x_g as

$$x_{g+1} = x_g - \bar{\lambda}. \quad (\text{A5})$$

Notice that $M'(x)$ is given by $M'(x) = ite^{ix}C + 2t \sin(x)$ with E given by Eq. (4). This is a diagonal matrix and can easily be inverted.

This iterative procedure has to start with a good initial

guess of x_g . In this paper, I use the complex eigenvalues E_i of the matrix $H'_{\text{GOE}} = H_{\text{GOE}} - i\Gamma/2$ and convert them to $x_g^{(i)} = \cos^{-1}(E_i/2t)$.

-
- [1] L. J. Patterson, H. Winkler, and C. S. Zaidins, *Astrophys. J.* **157**, 367 (1969).
- [2] D. G. Kovar, D. F. Geesaman, T. H. Braid, Y. Eisen, W. Henning, T. R. Ophel, M. Paul, K. E. Rehm, S. J. Sanders, P. Sperr, J. P. Schiffer, S. L. Tabor, S. Vigdor, B. Zeidman, and F. W. Prosser, Jr., *Phys. Rev. C* **20**, 1305 (1979).
- [3] L. J. Satkowiak, P. A. DeYoung, J. J. Kolata, and M. A. Xapsos, *Phys. Rev. C* **26**, 2027 (1982).
- [4] M. D. High and B. Cujec, *Nucl. Phys.* **A282**, 181 (1977).
- [5] M. Notani, H. Esbensen, X. Fang, B. Bucher, P. Davies, C. L. Jiang, L. Lamm, C. J. Lin, C. Ma, E. Martin, K. E. Rehm, W. P. Tan, S. Thomas, X. D. Tang, and E. Brown, *Phys. Rev. C* **85**, 014607 (2012).
- [6] N.T. Zhang, X.Y. Wang, D. Tudor, B. Bucher, I. Burducea, H. Chen, Z.J. Chen, D. Chesneanu, A.I. Chilug, L.R. Gasques, D.G. Ghita, C. Gomoiu, K. Hagino, S. Kubono, Y.J. Li, C.J. Lin, W.P. Lin, R. Margineanu, A. Pantelica, I.C. Stefanescu, M. Straticiuc, X.D. Tang, L. Trache, A.S. Umar, W.Y. Xin, S.W. Xu, and Y. Xu, *Phys. Lett.* **B801**, 135170 (2020).
- [7] T. Spillane, F. Raiola, C. Rolfs, D. Schürmann, F. Strieder, S. Zeng, H.-W. Becker, C. Bordeanu, L. Gialanella, M. Romano, and J. Schweitzer, *Phys. Rev. Lett.* **98**, 122501 (2007).
- [8] W. P. Tan, A. Boeltzig, C. Dulal, R. J. deBoer, B. Frenztz, S. Henderson, K. B. Howard, R. Kelmar, J. J. Kolata, E. F. Aguilera, P. Amador-Valenzuela, D. Lizcano, E. Martinez-Quiroz, J. Long, K. T. Macon, S. Moylan, G. F. Peaslee, M. Renaud, C. Seymour, G. Seymour, B. Vande Kolk, and M. Wiescher, *Phys. Rev. Lett.* **124**, 192702 (2020).
- [9] G. Fruet, S. Courtin, M. Heine, D. G. Jenkins, P. Adsley, A. Brown, R. Canavan, W. N. Catford, E. Charon, D. Curien, S. Della Negra, J. Duprat, F. Hammache, J. Lesrel, G. Lotay, A. Meyer, D. Montanari, L. Morris, M. Moukaddam, J. Nippert, Zs. Podolyák, P. H. Regan, I. Ribaud, M. Richer, M. Rudigier, R. Shearman, N. de Séréville, and C. Stodel, *Phys. Rev. Lett.* **124**, 192701 (2020).
- [10] C. L. Jiang, B. B. Back, H. Esbensen, R. V. F. Janssens, K. E. Rehm, and R. J. Charity, *Phys. Rev. Lett.* **110**, 072701 (2013).
- [11] A. Tumino, C. Spitaleri, M. La Cognata, S. Cherubini, G. L. Guardo, M. Gulino, S. Hayakawa, I. Indelicato, L. Lamia, H. Petrascu, R. G. Pizzone, S. M. R. Puglia, G. G. Rapisarda, S. Romano, M. L. Sergi, R. Spartá, and L. Trache, *Nature* **557**, 687 (2018).
- [12] B. Imanishi, *Phys. Lett.* **27B**, 267 (1968).
- [13] B. Imanishi, *Nucl. Phys.* **A125**, 33 (1969).
- [14] Y. Kondo, T. Matsuse, and Y. Abe, *Prog. Theo. Phys.* **59**, 465 (1978).
- [15] W. Scheid, W. Greiner, R. Lemmer, *Phys. Rev. Lett.* **25**, 176 (1970).
- [16] H. -J. Fink, W. Scheid, and W. Greiner, *Nucl. Phys.* **A188**, 259 (1972).
- [17] H. Esbensen, X. Tang, and C.L. Jiang, *Phys. Rev. C* **84**, 064613 (2011).
- [18] M. Assuncao and P. Descouvemont, *Phys. Lett.* **B723**, 355 (2013).
- [19] A. Diaz-Torres and M. Wiesher, *Phys. Rev. C* **97**, 055802 (2018).
- [20] A. Bonasera and J. B. Natowitz, *Phys. Rev. C* **102**, 061602 (R) (2020).
- [21] Y. Taniguchi and M. Kimura, *Prog. Theor. Phys.* **823**, 136790 (2021).
- [22] P.A. Moldauer, *Phys. Rev.* **157**, 907 (1967).
- [23] P.A. Moldauer, *Phys. Rev.* **171**, 1164 (1968).
- [24] G.L. Celardo, F.M. Izrailev, V.G. Zelevinsky, and G.P. Berman, *Phys. Lett.* **B659**, 170 (2008).
- [25] P.A. Moldauer, *Phys. Rev.* **177**, 1841 (1969).
- [26] M. Simonius, *Phys. Lett.* **52B**, 279 (1974).
- [27] G.F. Bertsch and K. Hagino, *Phys. Rev. C* **107** 044615 (2023).
- [28] P. Fanto, G.F. Bertsch, and Y. Alhassid, *Phys. Rev. C* **98**, 014604 (2018).
- [29] G.F. Bertsch and W. Younes, *Ann. Phys.* **403** 68 (2019).
- [30] Y. Alhassid, G.F. Bertsch, and P. Fanto, *Ann. of Phys.* **419**, 168233 (2020).
- [31] Y. Alhassid, G.F. Bertsch, and P. Fanto, *Ann. of Phys.* **424**, 168381 (2021).
- [32] K. Hagino, *Phys. Rev. C* **109** 034611 (2024).
- [33] K. Hagino, K. Ogata, and A.M. Moro, *Prog. in Part. and Nucl. Phys.* **125**, 103951 (2022).
- [34] K. Hagino and N. Takigawa, *Prog. Theo. Phys.* **128**, 1061 (2012).
- [35] C.A. Bertulani and P. Danelewicz, "Introduction to Nuclear Reactions" (CRC Press, Boca Raton, 2004).